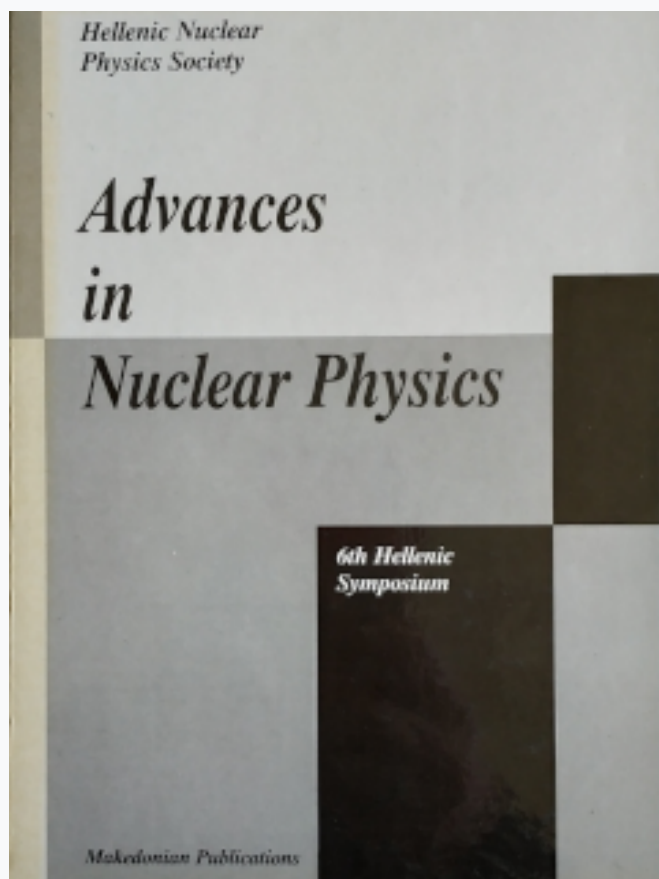


## HNPS Advances in Nuclear Physics

Vol 6 (1995)

HNPS1995



### Nuclear shape coexistence in $^{193}\text{Hg}$

*N. Fotiades, - et al.*

doi: [10.12681/hnps.2922](https://doi.org/10.12681/hnps.2922)

#### To cite this article:

Fotiades, N., & et al., .-. (2020). Nuclear shape coexistence in  $^{193}\text{Hg}$ . *HNPS Advances in Nuclear Physics*, 6, 131–139.  
<https://doi.org/10.12681/hnps.2922>

# Nuclear shape coexistence in $^{193}\text{Hg}$

N. Fotiades<sup>a</sup>, S. Harissopoulos<sup>a</sup>, C.A. Kalfas<sup>a</sup>, S. Kossionides<sup>a</sup>, C.T. Papadopoulos<sup>b</sup>, R. Vlastou<sup>b</sup>, M. Serris<sup>b</sup>, M. Meyer<sup>c</sup>, N. Redon<sup>c</sup>, R. Duffait<sup>c</sup>, Y. Le Coz<sup>c</sup>, L. Ducroux<sup>c</sup>, F. Hannachi<sup>d</sup>, I. Deloncle<sup>d</sup>, B. Gall<sup>d</sup>, M.G. Porquet<sup>d</sup>, C. Schuck<sup>d</sup>, F. Azaiez<sup>e</sup>, J. Duprat<sup>e</sup>, A. Korichi<sup>e</sup>, J.F. Sharpey-Schafer<sup>f</sup>, M.J. Joyce<sup>f</sup>, C.W. Beausang<sup>f</sup>, P.J. Dagnall<sup>f</sup>, P.D. Forsyth<sup>f</sup>, S.J. Gale<sup>f</sup>, P.M. Jones<sup>f</sup>, E.S. Paul<sup>f</sup>, J. Simpson<sup>g</sup>, R.M. Clark<sup>h</sup>, K. Hauschild<sup>h</sup> and R. Wadsworth<sup>h</sup>

<sup>a</sup>Inst. of Nuclear Physics, NCSR Demokritos, 15310 Athens, Greece

<sup>b</sup>National Technical University of Athens, 15773 Athens, Greece

<sup>c</sup>IPN de Lyon, Univ. Claude Bernard, F-69622 Villeurbanne Cedex, France

<sup>d</sup>CSNSM, IN2P3-CNRS, F-91405 Orsay Campus, France

<sup>e</sup>IPN, IN2P3-CNRS, F-91406 Orsay Campus, France

<sup>f</sup>Oliver Lodge Lab., Univ. of Liverpool, Liverpool L69 3BX, U.K.

<sup>g</sup>Daresbury Lab., Warrington WA4 4AD, U.K.

<sup>h</sup>Dept. of Physics, Univ. of York, York YO1 5DD, U.K.

---

## Abstract

Excited states of the  $^{193}\text{Hg}$  nucleus have been investigated by the reaction  $^{150}\text{Nd}$  ( $^{48}\text{Ca}, 5\text{n}$ ) at a beam energy of 213 MeV. The level scheme has been extended up to 10.7 MeV. Three different level pattern regions have been identified. A lower region with rotational bands, an intermediate region with single-particle character and an upper region with sequences of dipole transitions. The nature and the corresponding nuclear shape in these regions are discussed and compared with similar phenomena in the neighbouring nuclei.

---

## 1 Introduction

The low-lying level scheme of  $^{193}\text{Hg}$  isotope is well-known from previous experiments [1-7]. It consists mainly of sequences of E2 transitions interpreted as rotational bands built on various rotation-aligned quasi-neutron configurations [2]. Furthermore, the phenomenon of superdeformation has been recently

observed in this isotope [3]. Finally, recent investigations show that the level pattern of this isotope at higher excitation energies reveals a different behaviour from the collective rotation [6].

Recently, intense dipole bands were reported in the neighbouring Pb isotopes [8-19] as well as in  $^{192}\text{Hg}$  [20] and in  $^{196}\text{Hg}$  [21] consisting of dipole transitions, suggested as M1, with regular and irregular sequences. Weak crossover quadrupole transitions are observed to compete with the M1 transitions in some dipole bands in Pb isotopes and in all bands in Hg isotopes. The band-head excitation energy of these structures, still unknown in most of the cases, is expected to be a moderate one (4-6 MeV). Large  $B(\text{M1})/B(\text{E2})$  ratios are a common feature in the levels of dipole bands. However, larger  $B(\text{M1})/B(\text{E2})$  ratios are measured in the Pb nuclei ( $10-40\mu^2/(eb)^2$ ) than in the Hg nuclei ( $2-6\mu^2/(eb)^2$ ), a difference rendered to different intrinsic structures [21] in these isotopes. The interpretation of all dipole bands is based on high-K configurations involving  $h_{9/2}$  and  $i_{13/2}$  proton orbitals coupled to the neutron configurations of lower angular momenta. All these bands are suggested to emanate from a triaxial near-oblate nucleus rotating weakly collectively.

In  $^{191}\text{Hg}$  [22] a prolate deformed nuclear shape has been invoked for the interpretation of an irregular  $\gamma$ -ray sequence.  $\pi h_{11/2}$ ,  $\nu i_{13/2}$  and  $\nu h_{9/2}$  high-J orbitals change the nuclear shape from oblate collective towards the non-collective prolate. The  $\pi h_{11/2}$  orbital lies below the  $Z=80$  proton gap and hence is energetically favoured from the  $\pi h_{9/2}$  and  $\pi i_{13/2}$  excitations used in the dipole bands.

Here, we give evidence for three different level pattern regions existing in  $^{193}\text{Hg}$ . The previously known lower region with rotational bands, an intermediate region with single-particle character and an upper region with three dipole bands. The most important contribution of this work is perhaps the fact that we managed to precisely determine the excitation energy of all these regions and, by relating them to different nuclear shapes, we can deduce the regions of excitation energy where the nucleus changes its shape. The various  $\gamma$ -ray sequences in these regions are compared with the similar sequences in the neighbouring Pb and Hg isotopes.

## 2 Experimental Procedure

The  $^{150}\text{Nd}$  ( $^{48}\text{Ca},5\text{n}$ )  $^{193}\text{Hg}$  reaction, at beam energy  $E(^{48}\text{Ca}) = 213$  MeV, was used to populate high-spin states of  $^{193}\text{Hg}$  by means of the 20 MV tandem Van de Graaff accelerator at the NSF at Daresbury (UK). The target consisted of two stacked self-supporting foils of isotopically enriched  $^{150}\text{Nd}$  of thickness 500  $\mu\text{g}/\text{cm}^2$ . The EUROGAM detector array [23] was used to detect coincidences

between  $\gamma$ -rays from the reaction. Approximately  $10^9$  coincident events, of unsuppressed fold five or higher, were collected. From these events several two-dimensional  $4096 \times 4096$  channel matrices were built. One of them was symmetrized and used to investigate the coincidence relationships between the  $\gamma$ -rays. A second matrix was built to establish the directional correlations of the  $\gamma$ -rays  $I(158^\circ - 90^\circ)/I(90^\circ - 158^\circ)$ , where  $I(\theta_1 - \theta_2)$  is the intensity of  $\gamma$ -rays recorded by a detector at angle  $\theta_1$  while gated on a detector at angle  $\theta_2$  (DCO ratio). The rest of matrices were especially built from triples or quadruples to "filter" the regions of the level scheme at high excitations.

### 3 Results and discussion

In Fig. 1 a partial level scheme shows the deexcitation paths of  $^{193}\text{Hg}$  as established in this work. From the low-lying level scheme we included only the part that is in coincidence with the levels observed at higher excitations. Further information for the low-lying level scheme are given in ref. [1-7]. Here, we note that this part consists of several rotational bands and the shape of the nucleus is oblate.

Looking at the partial level scheme in Fig. 1 we can clearly identify three different regions:

- a lower region governed by bands of E2 transitions and extending up to approximately 4.5 MeV. Rotational bands govern the low-lying level scheme of all neighbouring Hg isotopes [2];
- an intermediate region of complicated level pattern extending up to approximately 7.0 MeV. A similar sequence has been reported in  $^{191}\text{Hg}$  [22];
- an upper region with three dipole bands, extending up to approximately 10.0 MeV. Dipole bands have also been reported in  $^{192}\text{Hg}$  [20],  $^{196}\text{Hg}$  [21] as well as in Pb [8-19] isotopes.

The limits of these regions can not be strictly defined since there is a certain overlapping between them, e.g. in the case of the deexcitation out of dipole bands 1 and 2 the complicated level pattern holds down to 2.0 MeV (see Fig. 1). This indicates that the various phenomena generating these regions can coexist.

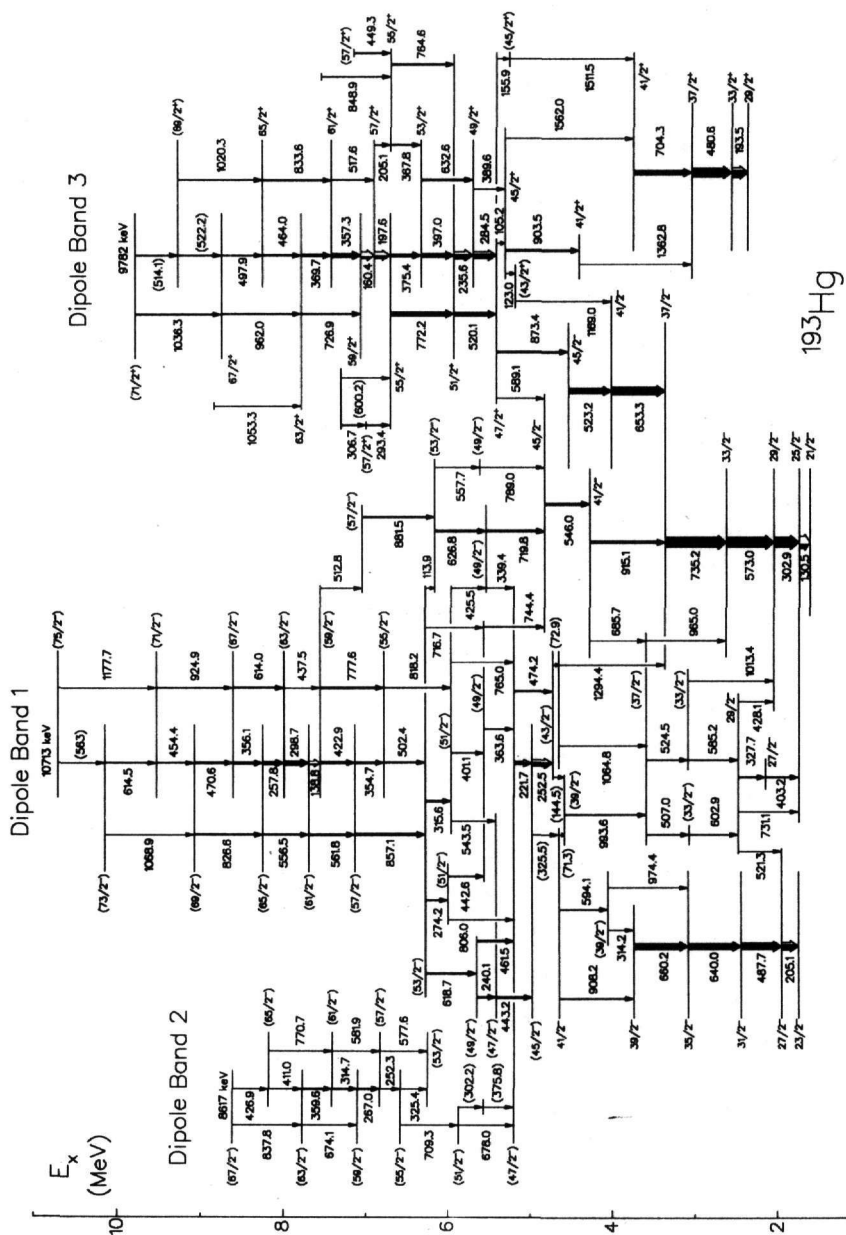


Fig. 1 : Partial level scheme of  $^{193}\text{Hg}$  obtained in the present work. The width of the arrows represents the intensity of the  $\gamma$ -rays. Excitation and  $\gamma$ -ray energies are in keV. Transitions, spins and parities in brackets are not firmly established.

In Total Routhian Surface (TRS) calculations performed for Hg isotopes the presence of high- $\Omega$  proton orbitals in the configurations proposed for the dipole bands drives the nucleus to a triaxial near-oblate, weakly collective shape ( $\gamma=-75^\circ$ ) [4,21]. On the other hand, the single-particle structure in  $^{191}\text{Hg}$  has been connected to a shape change towards a prolate non-collective shape ( $\gamma=-120^\circ$ ) [22]. Based on the similarities of the intermediate and upper regions of the  $^{193}\text{Hg}$  isotope to the single-particle structure in  $^{191}\text{Hg}$  and the dipole bands in the neighbouring isotopes, respectively, we can suggest similar shape changes for these regions in  $^{193}\text{Hg}$ . Hence, we propose a shape change from collective oblate in the lower region towards non-collective prolate in the intermediate region and triaxial near-oblate in the upper region. This scenario is in accordance with the theoretical calculations reported in [24] for  $^{194}\text{Hg}$ , but valid also for all neighbouring Hg isotopes. Indeed, these calculations predict a successive shape change from oblate collective ( $\gamma=-65^\circ$ ) towards prolate non-collective ( $\gamma=-120^\circ$ ) and triaxial weakly collective ( $\gamma=-80^\circ$ ), before the prolate ( $\gamma=0^\circ$ ) superdeformed minimum becomes yrast.

In order to search for possible configurations for the interpretation of the three dipole bands in the upper region we can compare the  $B(\text{M1})/B(\text{E2})$  ratios we measured experimentally for the levels of the dipole bands with theoretically calculated  $B(\text{M1})/B(\text{E2})$  ratios for various possible configurations in  $^{193}\text{Hg}$ . The experimentally measured  $B(\text{M1})/B(\text{E2})$  ratios were found to vary between 2 and  $4 \mu^2/(eb)^2$ . The model used in the theoretical calculations was the one introduced by Dönau and Frauendorf [25]. Both experimental points and theoretical curves are plotted in Fig. 2(i) for dipole bands 1 and 2 and in Fig. 2(ii) for dipole band 3.

The theoretical calculations of the  $B(\text{M1})/B(\text{E2})$  ratios have been carried out for four configurations. Based on the general conclusions of the previous works tackling the dipole bands in the neighbouring Hg [20,21] and Pb [8-19] isotopes, we choose high-K proton configurations coupled to high-J neutron orbitals. More specifically, we choose two deformation-aligned  $h_{9/2}$  and  $i_{13/2}$  proton orbitals coupled to aligned  $i_{13/2}$  neutrons. In  $^{192}\text{Hg}$ , four-neutron configurations have been successfully used in the interpretation of the dipole bands in this isotope [20]. It is therefore reasonable to use one more neutron in the corresponding configurations in  $^{193}\text{Hg}$ . Moreover, we need five neutrons in order to reproduce high angular momenta which characterize the states of the dipole bands. Thus, two of the four configurations (those labelled as a and c in Fig. 2) used in the calculations are  $\pi h_{9/2} i_{13/2} \otimes \nu i_{13/2}^5$  and  $\pi h_{9/2}^2 \otimes \nu i_{13/2}^5$ . Fully aligned nucleons have been assumed in all calculations, i.e.  $K=11$  and  $K=8$  for the mixed  $\pi(h_{9/2} i_{13/2})$  and the pure  $\pi(h_{9/2}^2)$  proton configurations, respectively, and  $i_c=22.5\hbar$  for the five neutrons. A quadrupole moment  $Q = -4.06\hbar^2$  (an oblate  $\beta = 0.136$  deformation) has been used. The collective gyromagnetic factor was taken equal to  $g_R = Z/A = 0.415$ , while for the mixed and pure proton configurations the values  $g=0.96$  [26] and  $g=0.78$  [19] were used.

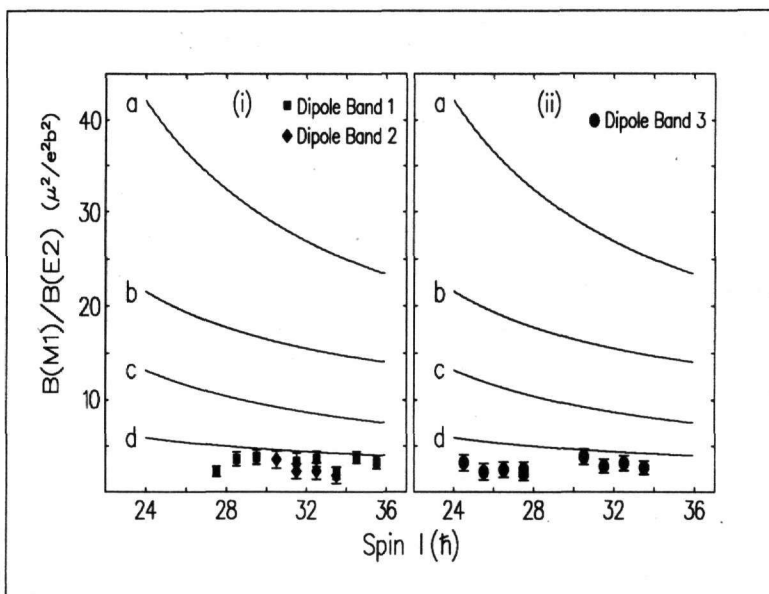


Fig. 2 : Experimental  $B(M1)/B(E2)$  values for some of the levels in dipole bands 1 (squares), 2 (diamonds) and 3 (circles). Solid lines represent theoretical calculations for various configurations (a, b, c and d represent the configurations  $\pi h_{9/2} i_{13/2} \otimes \nu i_{13/2}^5$ ,  $\pi h_{9/2} i_{13/2} h_{11/2}^{-2} \otimes \nu i_{13/2}^3$ ,  $\pi h_{9/2}^2 \otimes \nu i_{13/2}^5$ , and  $\pi h_{9/2}^2 h_{11/2}^{-2} \otimes \nu i_{13/2}^3$  respectively).

The  $B(M1)/B(E2)$  values for configurations a and c are rather large compared to the experimentally deduced values (see Fig. 2). In order to quench them,  $h_{11/2}$  proton holes can be used. Such excitations have already been applied to the configurations of the dipole bands in  $^{192}\text{Hg}$  [20] and  $^{196}\text{Hg}$  [21]. Thus, in two of the four configurations (those labelled as b and d in Fig. 2) two fully aligned  $h_{11/2}$  proton holes ( $i_x=10\hbar$ ) have been used instead of two  $i_{13/2}$  neutrons. The corresponding configurations are  $\pi h_{9/2} i_{13/2} \otimes \pi h_{11/2}^{-2} \otimes \nu i_{13/2}^3$  and  $\pi h_{9/2}^2 \otimes \pi h_{11/2}^{-2} \otimes \nu i_{13/2}^3$ . The quenching in the case of configuration b is not enough to bring the values close to the experimental points, while for configuration d the quenching reproduces the experimental values successfully. Hence, we suggest the latter configuration (d) as possible for the interpretation of the three dipole bands. This configuration is similar to the configurations used in the dipole bands of  $^{192}\text{Hg}$  [20] and  $^{196}\text{Hg}$  [21], but different from those

used in the Pb nuclei [8-19] which do not involve rotation-aligned proton holes. This indicates that the dipole bands have a different intrinsic structure in Hg isotopes from those in the Pb nuclei. Contribution of  $p_{3/2}$  neutrons in the case of dipole bands 1 and 2 is possible (because these structures have a negative parity) although since this orbital adds little alignment it has been considered as negligible in the calculations of the  $B(M1)/B(E2)$  ratio.

The difference of the  $B(M1)/B(E2)$  ratios for the dipole bands in  $^{193}\text{Hg}$  and Pb isotopes could be also attributed to different deformation effects. However, TRS calculations performed for  $^{193}\text{Hg}$  in ref. [4] predict weakly-deformed oblate shapes similar to the ones reported in Pb nuclei. The similarity between the nuclear shapes of these isotopes can only account for a small fraction of the difference in the experimental  $B(M1)/B(E2)$  ratios. Hence, we conclude that the one order of magnitude difference in the  $B(M1)/B(E2)$  ratios can only be accounted for by different intrinsic configurations.

In the few cases where the excitation energy of the dipole bands has been experimentally determined larger excitation energies were found in the Hg isotopes [20, present work] than in the Pb isotopes [8,15,17]. The use of  $h_{11/2}$  proton holes in the configurations of the Hg isotopes could qualitatively explain this difference. Indeed, in Pb isotopes the high-K  $h_{9/2}$  and  $i_{13/2}$  proton orbitals are occupied from proton excitations originating from the  $s_{1/2}$  orbital (see Fig. 3). Since more energy is needed to excite protons from the  $h_{11/2}$  orbital in the high-K orbitals than from the  $s_{1/2}$  orbital, we expect the configurations involving  $h_{11/2}$  proton holes in Hg to appear at higher excitation energies.

#### 4 Conclusions

In summary, the level scheme in  $^{193}\text{Hg}$  has been extended up to 10.7 MeV excitation energy. Three different regions (lower, intermediate and upper) were clearly identified. Comparison with similar situations in neighbouring isotopes and the theoretical predictions for the shape change in the Hg isotopes lead us to propose a shape change from collective oblate in the lower region towards non-collective prolate in the intermediate region and triaxial near-oblate in the upper region. The successive shape changes proposed for this isotope render it one of the most “ $\gamma$ -soft” nuclei in this atomic-mass region. The configurations proposed for the three dipole bands in the upper region, as well as for the dipole bands in the neighbouring Hg isotopes, are different from those suggested for the dipole bands in the neighbouring Pb isotopes, since they involve aligned  $h_{11/2}$  protons holes. This indicates different intrinsic structures in Hg and Pb nuclei, while the possibility of different deformations in these isotopes is minimized by TRS calculations.

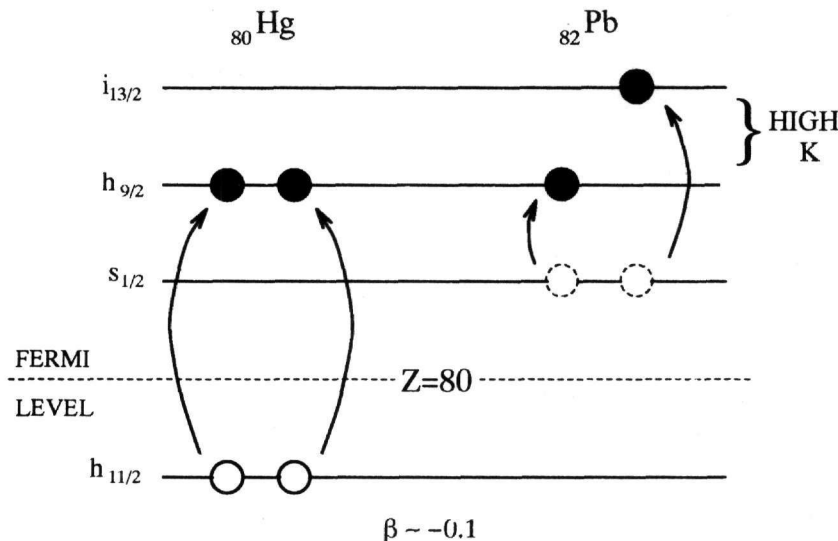


Fig. 3 : Proton orbitals involved in the configurations of the dipole bands in Hg and Pb isotopes.

## 5 Acknowledgments

We wish to thank the crew and technical staff at the, now defunct, NSF at Daresbury for excellent collaboration. The EUROGAM project is supported jointly by SERC (UK) and IN2P3 (France). One of the authors (N.F.) acknowledges the receipt of an NCNS Demokritos postgraduate studentship and another five (M.J.J., P.J.D., S.J.G., P.M.J. and R.M.C.) an SERC post-graduate studentship during the course of this work. The authors aknowledge support from EU (contract number SC1-CT91-687). Finally, J.S. acknowledges support from the NATO collaborative research programme.

## References

- [1] R M Lieder et al., Nucl. Phys. **A248** (1975)317
- [2] H Hübel et al., Nucl. Phys. **A453** (1986)316
- [3] D M Cullen et al., Phys. Rev. Lett. **65** (1990)1547
- [4] N Roy et al., Phys. Rev. **C47** (1993)R930

- [5] J K Deng et al., *Phys. Lett.* **B319** (1993)63
- [6] N Fotiades et al., Proceedings of the International conference on the future of Nuclear Spectroscopy, Crete (1993), INP NCSR Demokritos, 91
- [7] M J Joyce et al., *Phys. Rev. Lett.* **71** (1993)2176
- [8] B Fant et al., *J. Phys. G: Nucl. Part. Phys.* **17** (1991)319
- [9] A Kuhnert et al., *Phys. Rev.* **C46** (1992)133
- [10] T F Wang et al., *Phys. Rev. Lett.* **69** (1992)1737
- [11] G Baldsiefen et al., *Phys. Lett.* **B275** (1992)252
- [12] R M Clark et al., *Phys. Lett.* **B275** (1992)247
- [13] R M Clark et al., *Z. Phys.* **A342** (1992)371
- [14] G Baldsiefen et al., *Z. Phys.* **A343** (1992)245
- [15] G Baldsiefen et al., *Phys. Lett.* **B298** (1993)54
- [16] P J Dagnall et al., *J. of Phys.* **G19** (1993)465
- [17] J R Hughes et al., *Phys. Rev.* **C47** (1993)R1337
- [18] R M Clark et al., *Nucl. Phys.* **A562** (1993)121
- [19] R M Clark et al., *Phys. Rev.* **C50** (1994)84
- [20] Y Le Coz et al., *Z. Phys.* **A348** (1994)87
- [21] B Cederwall et al., *Phys. Rev.* **C47** (1993)R2443
- [22] D Ye et al., *Nucl. Phys.* **A537** (1992)207
- [23] C W Beausang et al., *NIM* **A313** (1992)37  
F.A. Beck, First biennial Workshop on Nuclear Physics, Megève, France, ed. D. Guinet and J.R. Pijji (World Scientific, 1991) p.365
- [24] M A Riley et al., *Nucl. Phys.* **A512** (1990)178
- [25] F Dönau and S Frauendorf, Proceedings of the Conference on High Angular Momentum Properties of Nuclei, Oak Ridge, (1982)143
- [26] J Penninga et al., *Nucl. Phys.* **A471** (1987)535